

## Henry's Law constants of 15 per- and polyfluoroalkyl substances determined by static headspace analysis

Ibrahim Abusallout <sup>a,b</sup>, Chase Holton <sup>c</sup>, Junli Wang <sup>b</sup>, David Hanigan <sup>b,\*</sup>

<sup>a</sup> CDM Smith, 14432 SE Eastgate Way Suite 100, Bellevue, WA, 98007, USA

<sup>b</sup> Department of Civil and Environmental Engineering, University of Nevada, Reno, NV 89557-0258, USA

<sup>c</sup> Geosyntec Consultants, Greenwood Village, CO 80111, USA

### ARTICLE INFO

#### Keywords:

PFAS  
Volatility  
Gas-phase  
Vapor intrusion  
Air-water partitioning

### ABSTRACT

While it is thought that some per- and polyfluoroalkyl substances (PFAS) may volatilize from aqueous solutions, experimentally measured Henry's Law constants ( $k_H$ , synonymous with air : water partition coefficient) are scarce. This leads to a lack of understanding of the partitioning of PFAS and an inability to predict concentrations above contaminated groundwater (e.g., vapor intrusion). We measured  $k_H$  for 27 PFAS via headspace analysis and manipulations of the gas to liquid phase ratio. Fifteen PFAS produced mass spectrometry signals suitable for  $k_H$  measurements. At 25 °C the experimentally measured dimensionless  $k_H$  were: 0.31 – 2.82 for four fluorotelomer alcohols (FTOHs), 0.09 – 0.18 for three fluorotelomer sulfonates (FTSs), 0.30 – 1.01 for three iodinated PFAS, 0.43 – 0.92 for two sulfonamides, 3.86 for 6:2 fluorotelomer olefin, 0.69 for 8:2 fluorotelomer carboxylic acid, and 0.32 for 8:2 fluorotelomer acrylate. Longer fluoroalkyl chain length resulted in increased  $k_H$  for FTOHs and FTSs, the only two groups in which chain length was studied. Perfluorinated sulfonates and carboxylates were generally not volatile enough to be measured, even at pH as low as 1, although fluorotelomers of both functional groups were measurably volatile. Temperature effects were well described by the van't Hoff equation.  $k_H$  was not significantly different in various environmentally relevant matrices demonstrating the broad applicability of the produced constants.

### 1. Introduction

Per- and polyfluoroalkyl substances (PFAS) are fluorinated organic chemicals that have unique chemical and mechanical attributes, including chemical and thermal stability. Thus, they have been used in a variety of industrial and commercial applications (Kissa, 2001). However, they are difficult to destroy, resulting in the nearly ubiquitous occurrence of PFAS across the globe, from the deep sea to arctic air (Yamashita et al., 2008; Shoeib et al., 2006), and human blood at microgram per liter concentrations (Worley et al., 2017; Hansen et al., 2001; Wang et al., 2018; Kwok et al., 2013; Munoz et al., 2017; Rahman et al., 2014; Xiao, 2017; Sinclair and Kannan, 2006). Exposure to PFAS has been shown to lead to adverse health outcomes in humans (Sunderland et al., 2019) and other ecological endpoints (Rericha et al., 2021), which is thought to be at least partially due to PFAS binding with serum albumin and proteins, causing interference with the binding of fatty acids and other endogenous ligands (Shi et al., 2012; Martin et al., 2003; Ahrens et al., 2009; Luebker et al., 2002).

A significant amount of research has focused on aqueous occurrence and transport of PFAS, but less is known about their release and occurrence to/in air. Among the published research focusing on gas-phase PFAS, indoor household air samples contained a total concentration of 3308  $\text{pg m}^{-3}$  of four gas phase PFAS (Shoeib et al., 2011). In another study, the concentration of PFAS in indoor household air samples (gas and particle phase) was 100 times higher than that found in outdoor urban air samples (Shoeib et al., 2004). Certain professions are also at greater risk of gas-phase PFAS exposure. For example, PFAS are used in some ski waxes and 19 perfluorinated carboxylic acids (PFCAs) and sulfonates (PFSAs) were present in the serum of 13 professional ski tuners. Perfluorooctanoic acid (PFOA) was present at the greatest concentration in the tuners' blood and ranged between 50 and 80,000  $\text{ng mL}^{-1}$  serum, potentially through the transformation of other PFAS in the air (Nilsson et al., 2010; Freberg et al., 2010). For example, the room air in which the employees worked contained 830 – 255,000  $\text{ng m}^{-3}$  8:2 fluorotelomer alcohol (FTOH) from the wax powder. Furthermore, our team recently published an investigation of PFAS present in the

\* Corresponding author.

E-mail address: [dhanigan@unr.edu](mailto:dhanigan@unr.edu) (D. Hanigan).

headspace above dilute, mildly agitated aqueous film-forming foam (AFFF) mixture and found a significant presence of organofluorine in the gas or aerosol phase (Roth et al., 2020).

Despite significant evidence of PFAS presence in the gas phase (Shoeib et al., 2006; Li et al., 2011; Dimzon et al., 2017; Ahrens et al., 2011; Weinberg et al., 2011; Gawor et al., 2014; Dreyer and Ebinghaus, 2009; Zhao et al., 2017; Jahnke et al., 2007; Rewerts et al., 2018; Wang et al., 2022; Morales-McDevitt et al., 2021), measurements of their Henry's Law constants ( $k_H$ , synonymous with air : water partition coefficient) are scarce (only FTOHs and PFCAs have published  $k_H$  data derived from experiments) (Kutsuna and Hori, 2008; Wu and Chang, 2011; Kwan, 2001; Goss et al., 2006; Lei et al., 2004). Some computational estimates are available but are highly variable (Lampic and Parinis, 2020). Together, these lead to a lack of understanding of PFAS partitioning and their potential to be a gas-phase health risk. Our goal was to assess the volatility of 27 PFAS and we provide measurements of  $k_H$  for 15 PFAS. The data allow for the development of fate and transport models, such as vapor intrusion models for PFAS contaminated groundwater, source attenuation and indoor air quality models, and provide insight into sources of atmospheric PFAS.

## 2. Methods and materials

$k_{HS}$  were measured similar to methods developed by Robbins, Wang and Stuart (Robbins et al., 1993) and Ettre, Welter and Kolb (Ettre et al., 1993) for low concentration contaminants in environmental matrices and validated by others (Miller and Stuart, 2000; Ramachandran et al., 1996). The method involves regressing the reciprocal peak areas produced by sample headspace injection into a gas chromatograph (GC) against varying sample headspace-to-water volume ratios. Briefly, in dilute solutions, partitioning to the gas phase to achieve equilibrium causes a corresponding decrease in the aqueous phase concentration. Thus, the equilibrium gas phase concentration is dependent on the gas to liquid phase ratio, with greater gas ratios causing increased losses from the liquid phase and subsequently reduced equilibrium gas phase concentrations. More volatile compounds are more susceptible to this phenomenon and the result is that the slope divided by the y-intercept of a reciprocal gas phase concentration vs gas to liquid ratio regression is the dimensionless  $k_H$ . GC peak area is directly proportional to concentration and therefore  $k_H$  can be derived by measuring the gas phase peak area of an individual compound at various phase ratios. The measurement is also independent of liquid phase concentration given that the concentration is sufficiently low. Further details of the derivation of this relationship and the required algebraic manipulations are provided in Ettre, Welter and Kolb (Ettre et al., 1993) and Robbins, Wang and Stuart (Robbins et al., 1993).

### 2.1. Sample preparation

A list of the 27 PFAS studied, including manufacturers and purity, is provided in Table S1 of the Supporting Information. Stock solutions were produced by dissolving each PFAS or up to four PFAS into methanol (MeOH). The methanol solutions were then diluted into Milli-Q water to make working solutions of  $2 \text{ mg PFAS L}^{-1}$ .  $2 \text{ mg PFAS L}^{-1}$  was selected to maximize the instrument signal, without exceeding the solubility (visually) of the compounds. This approach resulted in a 0.03 % (all PFAS except PFHxI and 10:2 FTOH) or 0.1 % (PFHxI and 10:2 FTOH) v/v cosolvent, and below  $\sim 1 \text{ % v/v}$  has been shown by others to have negligible impact on measurements of  $k_H$  (Schwarzenbach et al., 2005; Arp and Schmidt, 2004; Squillace et al., 1997; Ladaa et al., 2001). Samples were not buffered to avoid salting-out effects and thus the results for ionizable compounds are limited to a narrow pH range near the measured pH of the solution. pH was measured in triplicate and reported in Table 1 and ranged between 5.7 and 7.0. Headspace gas analysis vials (Shimadzu, Part No. 220-97331-10, Columbia, MD) were initially filled with the working solutions headspace-free, immediately capped, and

**Table 1**

PFAS  $k_H$  (dimensionless) measured at  $25 \text{ }^\circ\text{C}$  and at  $2 \text{ mg PFAS L}^{-1}$ . Compounds marked with asterisks have published experimental aqueous solubilities below the working solution concentration (Liu and Lee, 2007; Liu and Lee, 2005). Dissolution was facilitated with  $0.03 - 0.1 \text{ % MeOH}$ . 8:2 FTOH was repeated at a concentration lower than the aqueous solubility and there was not a statistically significant change in measured  $k_H$  (see Methods and materials, Table S3, Fig. S4), and the two  $k_H$  were the same or nearly the same as those measured using a different technique by others (Table S5). pH was not buffered to avoid salting-out effects and thus for ionizable compounds (FTSs, FOSAs, and 8:2 FTCA) these results should not be extended substantially beyond the measured pH. The uncertainty of the  $k_H$  estimates (standard deviation [SD] of single measurements of triplicate phase ratio vials) was determined with consideration of error propagation arising from uncertainties in both the slope and the y-intercept of the 1/peak area vs phase ratio linear best fit. All regressions had p-values less than 0.05.

PFAS	$k_H$	Slope	Intercept	$R^2$	pH
4:2 FTOH	$0.31 \pm$	$2.77 \pm 0.39$	$8.91 \pm 1.70 \times 10^{-5}$	0.920	$6.59 \pm 0.29$
	$0.07 \times 10^{-5}$				
6:2 FTOH	$1.26 \pm$	$5.18 \pm 0.29$	$4.12 \pm 1.20 \times 10^{-6}$	0.986	$6.55 \pm 0.08$
	$0.40 \times 10^{-6}$				
8:2 FTOH*	$1.98 \pm$	$1.51 \pm 0.06$	$7.66 \pm 2.60 \times 10^{-6}$	0.993	$6.74 \pm 0.17$
	$0.69 \times 10^{-5}$				
10:2 FTOH*	$2.82 \pm$	$6.92 \pm 0.22$	$2.45 \pm 0.96 \times 10^{-4}$	0.995	$6.69 \pm 0.26$
	$1.12 \times 10^{-4}$				
4:2 FTS	$0.09 \pm$	$4.11 \pm 0.88$	$4.33 \pm 0.38 \times 10^{-3}$	0.833	$5.66 \pm 0.02$
	$0.02 \times 10^{-4}$				
6:2 FTS	$0.16 \pm$	$2.37 \pm 0.17$	$1.48 \pm 0.08 \times 10^{-3}$	0.976	$5.70 \pm 0.01$
	$0.01 \times 10^{-4}$				
8:2 FTS	$0.18 \pm$	$8.55 \pm 0.65$	$4.75 \pm 0.28 \times 10^{-4}$	0.975	$5.84 \pm 0.03$
	$0.02 \times 10^{-5}$				
PFHxI	$1.01 \pm$	$4.70 \pm 0.47$	$4.66 \pm 2.01 \times 10^{-7}$	0.956	$6.90 \pm 0.01$
	$0.46 \times 10^{-7}$				
6:2 FTUI	$0.48 \pm$	$4.41 \pm 0.39$	$9.27 \pm 1.70 \times 10^{-6}$	0.966	$6.39 \pm 0.01$
	$0.10 \times 10^{-6}$				
6:2 FTI	$0.30 \pm$	$1.32 \pm 0.19$	$4.39 \pm 0.85 \times 10^{-6}$	0.910	$6.71 \pm 0.08$
	$0.07 \times 10^{-6}$				
N-EtFOSA-M	$0.43 \pm$	$1.18 \pm 0.15$	$2.77 \pm 0.68 \times 10^{-3}$	0.927	$6.33 \pm 0.16$
	$0.12 \times 10^{-3}$				
N-MeFOSA-M	$0.92 \pm$	$2.03 \pm 0.26$	$2.21 \pm 1.11 \times 10^{-3}$	0.933	$6.24 \pm 0.07$
	$0.48 \times 10^{-3}$				
6:2 FTO	$3.86 \pm$	$4.40 \pm 0.18$	$1.14 \pm 0.43 \times 10^{-7}$	0.987	$6.23 \pm 0.02$
	$1.49 \times 10^{-7}$				
8:2 FTCA	$0.69 \pm$	$8.18 \pm 0.26$	$1.19 \pm 0.11 \times 10^{-4}$	0.995	$5.66 \pm 0.28$
	$0.07 \times 10^{-5}$				
8:2 FTAC	$0.32 \pm$	$3.09 \pm 0.06$	$9.75 \pm 2.61 \times 10^{-4}$	0.858	$6.58 \pm 0.05$
	$0.11 \times 10^{-3}$				

placed into  $25 \text{ }^\circ\text{C}$  water bath for 5 min to reach temperature equilibrium. Five gas-to-liquid phase ratios (0.3, 1.0, 1.5, 3.0 and 9.0) were produced in triplicate by withdrawing a fixed volume of the stock solution using one needle, while allowing room air to backfill the headspace with another open-ended needle. Further details of the sample preparation procedure are provided in the Supporting Information. Once headspace was generated, vials were agitated for three minutes and inverted for an additional 30 min to achieve phase equilibrium. Phase equilibrium was confirmed by measuring the gas-phase peak area of 6:2 FTOH and PFHxI after equilibrating vials containing these individual compounds, at gas to liquid phase ratio of 9, for varying hold times at room temperature. Less than or equal to 30 min was necessary to obtain stable peak area (standard deviation  $< 10 \text{ %}$ ), and thus, phase equilibrium (Table S2).

To assess the assumption that aqueous phase concentrations were sufficiently low, measurements were repeated at  $100 \text{ } \mu\text{g L}^{-1}$  in the aqueous phase for three FTOHs, PFHxI and 6:2 FTO, and the resulting  $k_H$  (Table S3, Fig. S4) were not significantly different from those conducted at  $2 \text{ mg L}^{-1}$  (t-test,  $p > 0.05$ ).  $k_H$  for 4:2 FTOH and N-EtFOSA-M was also measured in tap water, wastewater, and groundwater to determine the effects of constituents found in environmentally relevant matrices. The spiked PFAS concentrations in these additional matrices were greater than the experiments in Milli-Q water ( $300 \text{ } \mu\text{g L}^{-1}$  vs  $100 \text{ } \mu\text{g L}^{-1}$ ) to facilitate GC-MS/MS analysis with greater interference from

background organic matter. In one limited set of experiments, the pH of the samples was adjusted to  $< 2$  using concentrated sulfuric acid and PFAS in the headspace was measured.

## 2.2. Analysis

Headspace gas was sampled by a Shimadzu AOC-6000 autosampler. Initially, samples were transferred to the sample heating block for 30 min. The heating block temperature was 25 °C unless otherwise stated. After equilibrating in the heating block, 1 mL of the headspace was collected using a GC headspace tool (Shimadzu Part NO. 220-94928-19) equipped with a 1 mL gas-tight syringe (Shimadzu Part NO. 220-94500-05) heated to 90 °C. The headspace sample was immediately injected into a GC-MS/MS (Shimadzu TQ8040).

Injected samples were chromatographically separated with a HP-5 column (30 m, 0.32 mm I.D., 0.25 μm film thickness). The injector port was set to 250 °C and 150 kPa, resulting in a column flow of 2.75 mL He min<sup>-1</sup>. The oven program was as follows: initial temperature held at 40 °C for 4 min, ramped to 220 °C at 15 °C min<sup>-1</sup> and held for 1 min. The MS interface temperature was 220 °C and the ion source temperature was set to 200 °C. Initial experiments were conducted to determine the most prominent parent and product ions resulting from the gas-phase PFAS. Argon was the collision gas. Selected ion fragments for each PFAS are included in Table S4 of the Supporting Information and generally were ions characteristic of fluorocarbons. Only peaks with greater than three times the signal to noise ratio (S:N) were included in the analysis.

A plot of 1/peak area vs headspace volume / water volume was developed for each PFAS. Linear least-squares best fits, Q-tests on outliers, averages, t- and F-tests, p-values, and uncertainty in the estimates of the regression coefficients (slope and y-intercept) were calculated with SigmaPlot v.14.5. A schematic of the experimental design, preparation, and analysis is shown in Fig. 1.

## 3. Results and discussion

### 3.1. Henry's Law constants

Initial experiments were conducted to assess the assumptions that the liquid phase concentration was sufficiently low and that phase equilibrium was achieved, and the results confirmed these assumptions

(see Methods and materials and the Supporting Information [Table S2]). Representative plots of 1/peak area vs phase ratio are presented in Fig. 2. Additional plots for the remaining 11 PFAS which were measurable are presented in the Supporting Information (Fig. S1–S3). A summary of  $k_H$  derived from these plots is presented in Table 1. Linear best fit regressions resulted in  $R^2 \geq 0.83$ . All regressions had p-values less than 0.05.  $k_H$  generally decreased in order of PFAS functional group as follows: FTOs > FTOHs > sulfonamides > iodinated ~ FTCA > FTAC > FTSS. Note that these comparisons are in some cases based on a single PFAS from the functional group. Additionally, the 2 mg PFAS L<sup>-1</sup> solutions are in some case in excess of the published aqueous solubility (See Table 1). When the working solutions were made directly, without the MeOH intermediate, it was visually apparent that several PFAS were not dissolved. However, first dissolving the PFAS in MeOH and then spiking the MeOH solution to Milli-Q water resulted in dissolution of all compounds. The effect of 0.03 – 0.1 % cosolvent has been demonstrated previously to have negligible impact on measurements of  $k_H$  (Schwarzenbach et al., 2005; Arp and Schmidt, 2004; Squillace et al., 1997; Ladaa et al., 2001). Twelve other PFAS including 7 PFCAs and 3 PFSA were not volatile enough or not ionized well enough in the mass spectrometer source to produce signals above the signal to noise threshold (3:1).

For the two groups in which multiple chain lengths were included (i.e., FTOHs and FTSS), increasing alkyl chain length resulted in greater  $k_H$ . For FTOHs, the only group in which there is comparable published literature, the effect of chain length on  $k_H$  is similar to another study using a gas stripping method of measuring  $k_H$  (Wu and Chang, 2011), but was less strong when compared to a third which measured  $k_H$  of only 4:2 FTOH and 6:2 FTOH (Goss et al., 2006) (Table S5). Iodinated PFAS have been reported to be volatile, are present in the lower atmosphere near carpet manufacturers, and our team has measured them in AFFF headspace, but no  $k_H$  have been previously reported. The finding that iodinated PFAS are volatile may explain their detection in the gas phase in various environmental compartments (Dimzon et al., 2017; Ruan et al., 2010; Kempisty et al., 2018).

Of the carboxylic acids, only 8:2 FTCA was detected in the gas phase. This lack of detection might be attributed to the low  $pK_a$  of fluorinated carboxylates which results in their occurrence as anions in environmental systems and in these unbuffered experiments. Kwan (Kwan, 2001) circumvented this by reducing the pH of the solution to  $< 2$  and was successful at determining experimental  $k_H$  for seven PFCAs. To

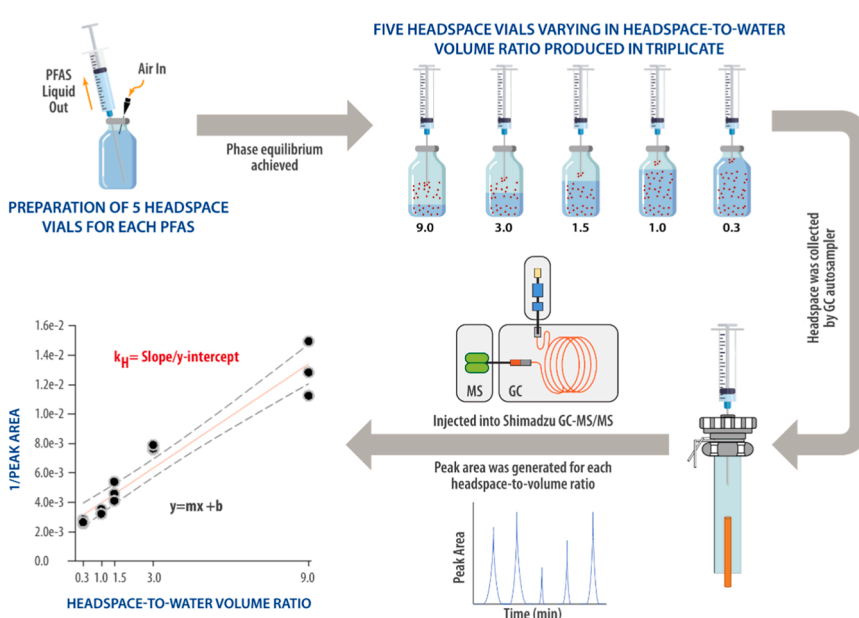
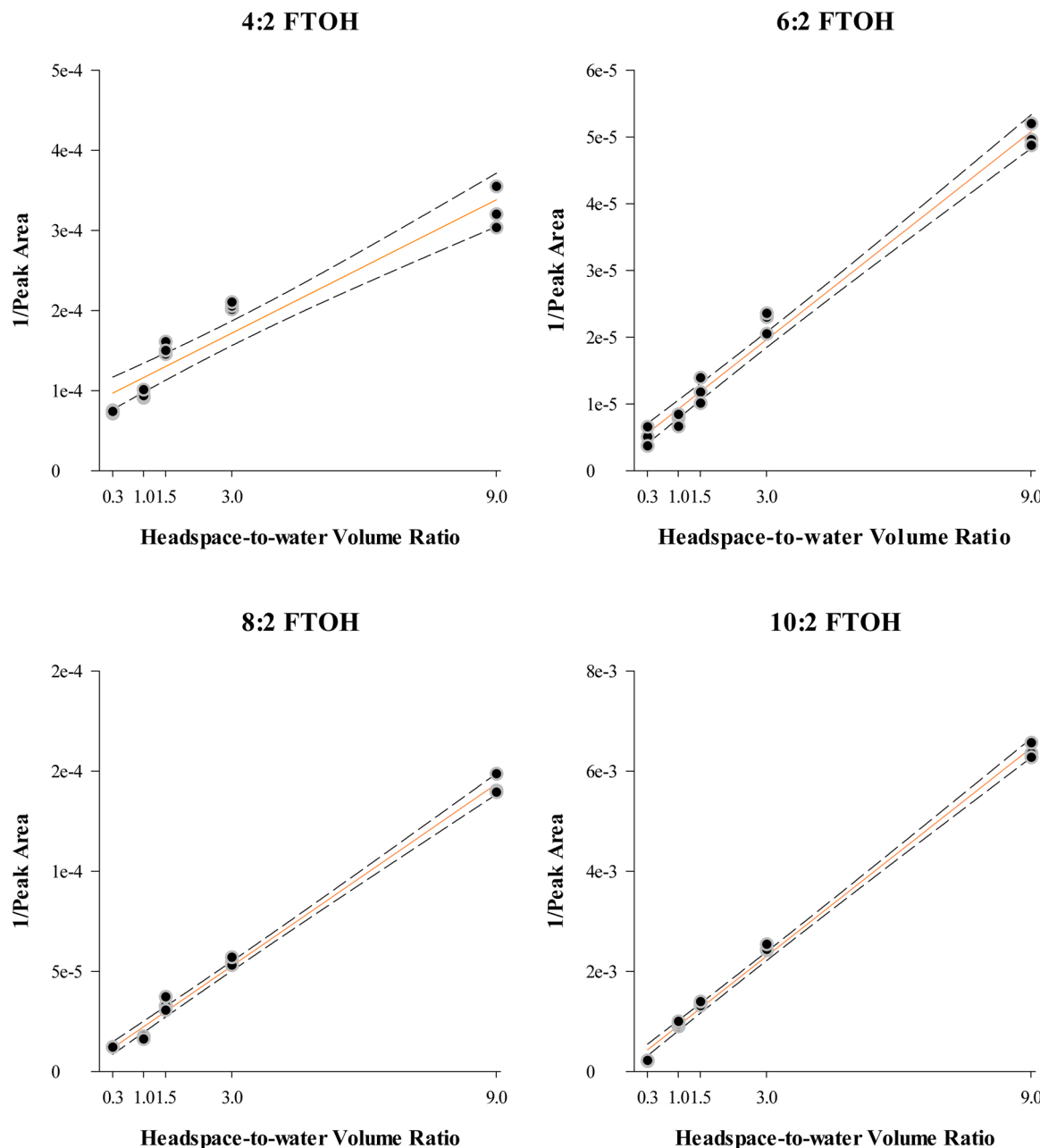


Fig. 1. Schematic of the method of preparing and analyzing headspace samples by GC-MS/MS for the determination of the  $k_H$  of PFAS.



**Fig. 2.** Representative plots used to derive Henry's Law Constants of four FTOHs. The solid line is the linear best fit, and the dashed lines are the 95 % confidence interval. The slope divided by the y-intercept is dimensionless  $k_H$ .

follow up on this, we reduced the pH of seven PFCAs and three PFSAs including PFPeA, PFBA, PFPeA, PFHpA, PFOA, PFNA and PFDA to 0.5, 1.0 and 2.0. No peaks were observed at pH 2. Peaks at pH 0.5 and 1.0 were observed only for PFHpA, PFOA, PFNA and PFDA but not greater than S:N of 3, and very early in the chromatogram (< 1 min). The  $pK_a$  of PFCAs is still an area of active debate with some literature finding  $pK_a < 1$  (Goss, 2008; Moroi et al., 2001) and another > 3 (Burns et al., 2008). This research suggests that the  $pK_a$ s of PFCAs are likely to be < 0. and because of this, PFCAs are unlikely to partition to the gas phase when they are present as anions. This is also likely true for PFSAs and explains the lack of gas phase detection in these experiments.

### 3.2. Temperature

We expected that temperature would impact PFAS  $k_H$  and we proceeded to investigate whether the relationship was described by the

van't Hoff equation. In Table 2, we present the impact of varying temperature on  $k_H$  of four PFAS between 25 and 50 °C. Only four PFAS were investigated over this relatively narrow range of temperatures because the goal was to demonstrate the expected relationship rather determine the coefficients. Linear correlation coefficients were obtained from the plots (Fig. S5) between natural log of PFAS  $k_H$  and the reciprocal of the temperature. Pearson correlation coefficients for 6:2 FTOH, 6:2 FTS, PFHxI and 6:2 FTO were > 0.97, demonstrating that PFAS  $k_H$  are well described by a van't Hoff type relationship. 6:2 FTS exhibited the greatest increase in  $k_H$  ~15 times increase at 50 °C compared to 25 °C, where 6:2 FTOH and 6:2 FTO exhibited the lowest decrease; ~3 times, over the same temperature range. These large differences of  $k_H$  with temperature can also be demonstrated by calculating internal energy of phase transition ( $\Delta U_{AW}$ ) of the four PFAS (Table 2). 6:2 FTS exhibited more than double  $\Delta U_{AW}$  compared to 6:2 FTOH and 6:2 FTO. Lei et al. (Lei et al., 2004) examined three FTOHs and observed similar  $\Delta U_{AW}$  of

**Table 2**

PFAS Henry's Law constants at a range of temperatures.  $\Delta U_{AW}$  values were calculated using the slopes generated from regression between  $1/T$  (1/K) and  $\ln k_H$  (dimensionless).

PFAS	$k_H$ (dimensionless)						$\ln k_H$ (atm m <sup>3</sup> mol <sup>-1</sup> ) vs $1/T$ (K) regression	$R^2$	$\Delta U_{AW}$ (kJ mol <sup>-1</sup> )
	25 °C	30 °C	35 °C	40 °C	45 °C	50 °C			
6:2 FTOH	1.25	1.50	1.89	2.50	3.00	3.90	$y = -4427.7x + 11.3$	0.995	36.8
6:2 FTS	0.16	0.38	0.59	1.24	2.09	2.34	$y = -10647.3x + 30.3$	0.972	88.5
PFHxI	1.00	1.25	1.89	3.11	5.00	7.00	$y = -7908.9x + 22.7$	0.988	65.8
6:2 FTO	3.90	4.94	5.77	8.13	10.43	12.44	$y = -4612.6x + 13.1$	0.990	38.4

phase transition for 6:2 FTOH (36.8 kJ mol<sup>-1</sup>). Kwan (Kwan, 2001) also examined PFCA  $k_H$  at varying temperatures (up to 50 °C) at pH < 2 and observed a similar dependence on temperature.

It is surprising that FTSs and 8:2 FTCA were measurable in the gas phase given their potentially low pK<sub>a</sub>s, although the strong  $k_H$  dependence on temperature for FTSs may indicate increased pK<sub>a</sub>s of the telomers acids compared to the perfluorinated acids given that temperature has a greater effect on the pK<sub>a</sub>s of weak over strong acids, resulting in a greater number of neutral molecules in solution and ultimately an increased temperature dependence of  $k_H$  (Schwarzenbach et al., 2005). Further, -CH<sub>2</sub>-CH<sub>2</sub>- is less electron withdrawing than -CF<sub>2</sub>-CF<sub>2</sub>- and it has been shown that this results in a substantially increased pK<sub>a</sub>, approaching that of non-fluorinated acids (Henne and Fox, 1951).

### 3.3. Natural water constituents

We proceeded to examine the impact of water matrix on  $k_H$ . We examined environmentally relevant matrices including two tertiary wastewater effluents, tap water produced by a conventional treatment plant treating surface water, and groundwater from a treatment zone monitoring well near an active U.S. Air Force base. Details about these waters and their characteristics are reported in Table S6 in the Supporting Information. No PFAS were detectable in the headspace before the analyte spikes.  $k_H$  were determined for two PFAS (4:2 FTOH and *N*-MeFOSA-M) at 25 °C. The results are shown in Fig. 3 and the linear correlation coefficients were obtained from the plots (Figs. S6, S7).  $k_H$  were not statistically different in the varying water matrices when compared to Milli-Q water ( $p > 0.05$ ) and thus the interactions between PFAS and constituents present in typical environmental samples had no significant effect on PFAS volatility. Therefore, it is expected that the reported  $k_H$  are applicable to a wide range of environmental matrices given that dissolved constituents are reasonably low.

We believe that these results will improve environmental practitioners' understanding of gas-phase PFAS sources and the potential for release of gas-phase PFAS from aqueous solutions, including AFFF and

contaminated groundwater or wastewater sources. The Henry's Law constants presented herein exceed the volatility criteria used by the U.S. Environmental Protection Agency used in identifying chemicals of potential vapor intrusion concern (i.e., compounds with  $k_H > 10^{-5}$  atm m<sup>3</sup> mol<sup>-1</sup> [4.1 × 10<sup>-4</sup> dimensionless, obtained by dividing  $k_H$  [atm m<sup>3</sup> mol<sup>-1</sup>] by the gas constant [ $R = 8.205 \times 10^{-5}$  atm m<sup>3</sup> mol<sup>-1</sup> K<sup>-1</sup>] and multiplying by 298 K] (USEPA, 2015). The potential risk of PFAS vapor intrusion into overlying buildings from impacted groundwater might be of concern near production facilities or other significant sources of volatile PFAS, and further investigation into the PFAS soil vapor to indoor air pathway is warranted.

### Declaration of Competing Interest

The authors declare that they have no known competing financial interests or personal relationships that could have appeared to influence the work reported in this paper.

### Data availability

Data will be made available on request.

### Acknowledgments

This research was supported by National Science Foundation Grants 2128407 and 2219833 and by the Strategic Environmental Research and Development Program Grant ER19-1214. Views, opinions, and/or findings contained in this report are those of the authors and should not be construed as an official Department of Defense position or decision unless so designated by other official documentation. The authors would like to thank Jacobs Engineering Group for providing the groundwater samples.

### Appendix A. Supporting information

Supplementary data associated with this article can be found in the online version at doi:10.1016/j.hazl.2022.100070.

### References

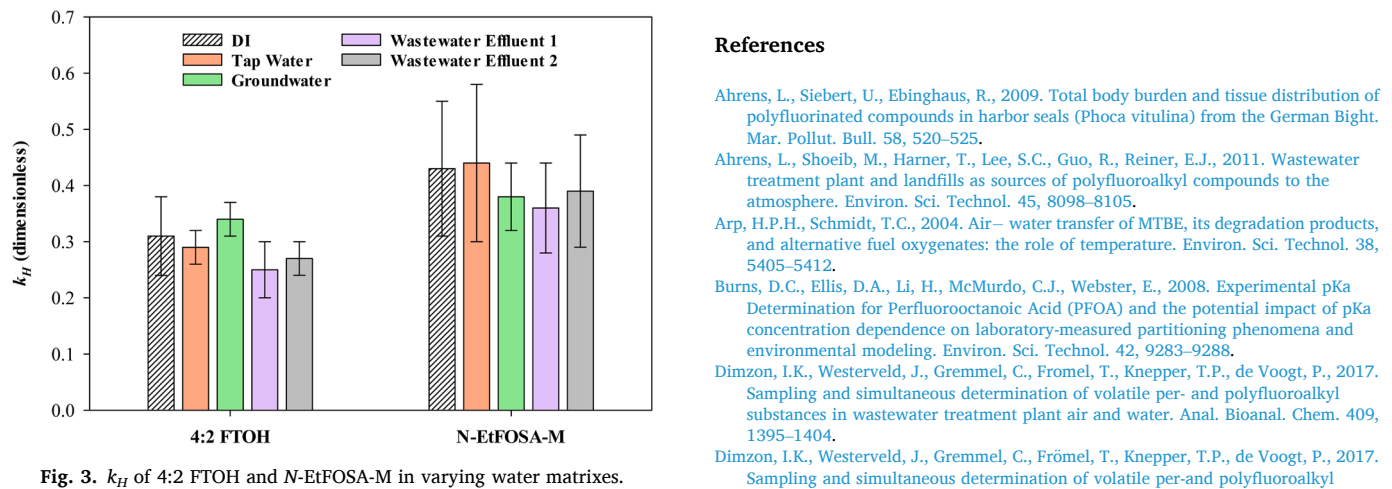


Fig. 3.  $k_H$  of 4:2 FTOH and *N*-EtFOSA-M in varying water matrixes.

substances in wastewater treatment plant air and water. *Anal. Bioanal. Chem.* 409, 1395–1404.

Dreyer, A., Ebinghaus, R., 2009. Polyfluorinated compounds in ambient air from ship- and land-based measurements in northern Germany. *Atmos. Environ.* 43, 1527–1535.

Ettrre, L., Welter, C., Kolb, B., 1993. Determination of gas-liquid partition coefficients by automatic equilibrium headspace-gas chromatography utilizing the phase ratio variation method. *Chromatographia* 35, 73–84.

Freberg, B.I., Haug, L.S., Olsen, R., Daae, H.L., Hersson, M., Thomsen, C., Thorud, S., Becher, G., Molander, P., Ellingsen, D.G., 2010. Occupational exposure to airborne perfluorinated compounds during professional ski waxing. *Environ. Sci. Technol.* 44, 7723–7728.

Gawor, A., Shunthirasingham, C., Hayward, S., Lei, Y., Gouin, T., Mmerek, B., Masamba, W., Ruepert, C., Castillo, L., Shoeib, M., 2014. Neutral polyfluoroalkyl substances in the global atmosphere. *Environ. Sci. Process. Impacts* 16, 404–413.

Goss, K.-U., 2008. The pKa values of PFOA and other highly fluorinated carboxylic acids. *Environ. Sci. Technol.* 42, 456–458.

Goss, K.-U., Bronner, G., Harner, T., Hertel, M., Schmidt, T.C., 2006. The partition behavior of fluorotelomer alcohols and olefins. *Environ. Sci. Technol.* 40, 3572–3577.

Hansen, K.J., Clemen, L.A., Ellefson, M.E., Johnson, H.O., 2001. Compound-specific, quantitative characterization of organic fluorochemicals in biological matrices. *Environ. Sci. Technol.* 35, 766–770.

Henne, A.L., Fox, C.J., 1951. Ionization constants of fluorinated acids. *J. Am. Chem. Soc.* 73, 2323–2325.

Jahnke, A., Ahrens, L., Ebinghaus, R., Berger, U., Barber, J.L., Temme, C., 2007. An improved method for the analysis of volatile polyfluorinated alkyl substances in environmental air samples. *Anal. Bioanal. Chem.* 387, 965–975.

Kempisty, D.M., Xing, Y., Racz, L., 2018. *Perfluoroalkyl Substances in the Environment: Theory, Practice, and Innovation*. CRC Press.

Kissa, E., 2001. *Fluorinated Surfactants and Repellents*. CRC Press.

Kutsuna, S., Hori, H., 2008. Experimental determination of Henry's law constant of perfluorooctanoic acid (PFOA) at 298 K by means of an inert-gas stripping method with a helical plate. *Atmos. Environ.* 42, 8883–8892.

W.C. Kwan, Physical property determination of perfluorinated surfactants, in, University of Toronto, 2001.

Kwok, K.Y., Yamazaki, E., Yamashita, N., Taniyasu, S., Murphy, M.B., Horii, Y., Petrick, G., Kallerborn, R., Kannan, K., Murano, K., Lam, P.K., 2013. Transport of perfluoroalkyl substances (PFAS) from an arctic glacier to downstream locations: implications for sources. *Sci. Total Environ.* 447, 46–55.

Ladaa, T.I., Lee, C.M., Coates, J.T., Falta Jr, R.W., 2001. Cosolvent effects of alcohols on the Henry's law constant and aqueous solubility of tetrachloroethylene (PCE). *Chemosphere* 44, 1137–1143.

Lampic, A., Parnis, J.M., 2020. Property estimation of per- and polyfluoroalkyl substances: a comparative assessment of estimation methods. *Environ. Toxicol. Chem.* 39, 775–786.

Lei, Y.D., Wania, F., Mathers, D., Mabury, S.A., 2004. Determination of vapor pressures, octanol–air, and water–air partition coefficients for polyfluorinated sulfonamide, sulfonamidoethanols, and telomer alcohols. *J. Chem. Eng. Data* 49, 1013–1022.

Li, J., Del Vento, S., Schuster, J., Zhang, G., Chakraborty, P., Kobara, Y., Jones, K.C., 2011. Perfluorinated compounds in the Asian atmosphere. *Environ. Sci. Technol.* 45, 7241–7248.

Liu, J., Lee, L.S., 2005. Solubility and sorption by soils of 8:2 fluorotelomer alcohol in water and cosolvent systems. *Environ. Sci. Technol.* 39, 7535–7540.

Liu, J., Lee, L.S., 2007. Effect of fluorotelomer alcohol chain length on aqueous solubility and sorption by soils. *Environ. Sci. Technol.* 41, 5357–5362.

Luebker, D.J., Hansen, K.J., Bass, N.M., Butenhoff, J.L., Seacat, A.M., 2002. Interactions of fluorochemicals with rat liver fatty acid-binding protein. *Toxicology* 176, 175–185.

Martin, J.W., Mabury, S.A., Solomon, K.R., Muir, D.C., 2003. Bioconcentration and tissue distribution of perfluorinated acids in rainbow trout (*Oncorhynchus mykiss*). *Environ. Toxicol. Chem.* 22, 196–204.

Miller, M.E., Stuart, J.D., 2000. Measurement of aqueous Henry's law constants for oxygenates and aromatics found in gasolines by the static headspace method. *Anal. Chem.* 72, 622–625.

Morales-McDevitt, M.E., Bocanova, J., Blum, A., Bruton, T.A., Vojta, S., Woodward, M., Lohmann, R., 2021. The Air That We Breathe: Neutral and Volatile PFAS in Indoor Air. *Environ. Sci. Technol. Lett.* 8, 897–902.

Moroi, Y., Yano, H., Shibata, O., Yonemitsu, T., 2001. Determination of acidity constants of perfluoroalkanoic acids. *Bull. Chem. Soc. Jpn.* 74, 667–672.

Munoz, G., Labadie, P., Botta, F., Lestremau, F., Lopez, B., Geneste, E., Pardon, P., Devier, M.H., Budzinski, H., 2017. Occurrence survey and spatial distribution of perfluoroalkyl and polyfluoroalkyl surfactants in groundwater, surface water, and sediments from tropical environments. *Sci. Total Environ.* 607–608, 243–252.

Nilsson, H., Kärrman, A., Westberg, H., Rotander, A., Van Bavel, B., Lindström, G., 2010. A time trend study of significantly elevated perfluorocarboxylate levels in humans after using fluorinated ski wax. *Environ. Sci. Technol.* 44, 2150–2155.

Rahman, M.F., Peldszus, S., Anderson, W.B., 2014. Behaviour and fate of perfluoroalkyl and polyfluoroalkyl substances (PFASs) in drinking water treatment: a review. *Water Res.* 50, 318–340.

Ramachandran, B., Allen, J.M., Halpern, A.M., 1996. The importance of weighted regression analysis in the determination of Henry's law constants by static headspace gas chromatography. *Anal. Chem.* 68, 281–286.

Reicher, Y., Cao, D., Truong, L., Simonich, M., Field, J.A., Tanguay, R.L., 2021. Behavior effects of structurally diverse per- and polyfluoroalkyl substances in zebrafish. *Chem. Res. Toxicol.*

Rewerts, J.N., Morre, J.T., Massey Simonich, S.L., Field, J.A., 2018. In-vial extraction large volume gas chromatography mass spectrometry for analysis of volatile PFASs on papers and textiles. *Environ. Sci. Technol.* 52, 10609–10616.

Robbins, G.A., Wang, S., Stuart, J.D., 1993. Using the static headspace method to determine Henry's law constants. *Anal. Chem.* 65, 3113–3118.

Roth, J., Abusallout, I., Hill, T., Holton, C., Thapa, U., Hanigan, D., 2020. Release of volatile per- and polyfluoroalkyl substances from aqueous film-forming foam. *Environ. Sci. Technol. Lett.* 7, 164–170.

Ruan, T., Wang, Y., Wang, T., Zhang, Q., Ding, L., Liu, J., Wang, C., Qu, G., Jiang, G., 2010. Presence and partitioning behavior of polyfluorinated iodine alkanes in environmental matrices around a fluorochemical manufacturing plant: another possible source for perfluorinated carboxylic acids? *Environ. Sci. Technol.* 44, 5755–5761.

Schwarzenbach, R.P., Gschwend, P.M., Imboden, D.M., 2005. *Environmental Organic Chemistry*. John Wiley & Sons.

Shi, Y., Wang, J., Pan, Y., Cai, Y., 2012. Tissue distribution of perfluorinated compounds in farmed freshwater fish and human exposure by consumption. *Environ. Toxicol. Chem.* 31, 717–723.

Shoeib, M., Harner, T., Ikonomou, M., Kannan, K., 2004. Indoor and outdoor air concentrations and phase partitioning of perfluoroalkyl sulfonamides and polybrominated diphenyl ethers. *Environ. Sci. Technol.* 38, 1313–1320.

Shoeib, M., Harner, T., Vlahos, P., 2006. Perfluorinated chemicals in the arctic atmosphere. *Environ. Sci. Technol.* 40, 7577–7583.

Shoeib, M., Harner, T., G, M.W., Lee, S.C., 2011. Indoor sources of poly- and perfluorinated compounds (PFCS) in Vancouver, Canada: implications for human exposure. *Environ. Sci. Technol.* 45, 7999–8005.

Sinclair, E., Kannan, K., 2006. Mass loading and fate of perfluoroalkyl surfactants in wastewater treatment plants. *Environ. Sci. Technol.* 40, 1408–1414.

Squillace, P.J., Pankow, J.F., Korte, N.E., Zogorski, J.S., 1997. Review of the environmental behavior and fate of methyl tert-butyl ether. *Environ. Toxicol. Chem.* Int. J. 16, 1836–1844.

Sunderland, E.M., Hu, X.C., Dassuncao, C., Tokranov, A.K., Wagner, C.C., Allen, J.G., 2019. A review of the pathways of human exposure to poly- and perfluoroalkyl substances (PFASs) and present understanding of health effects. *J. Expo. Sci. Environ. Epidemiol.* 29, 131–147.

USEPA, O.S.W.E.R. Technical Guide for Assessing and Mitigating the Vapor Intrusion Pathway from Subsurface Vapor Sources to Indoor Air, in, EPA Office of Solid Waste and Emergency Response Washington, DC, USA, 2015.

Wang, J., Pan, Y., Cui, Q., Yao, B., Wang, J., Dai, J., 2018. Penetration of PFASs across the blood cerebrospinal fluid barrier and its determinants in humans. *Environ. Sci. Technol.* 52, 13553–13561.

Wang, S., Lin, X., Li, Q., Liu, C., Li, Y., Wang, X., 2022. Neutral and ionizable per- and polyfluoroalkyl substances in the urban atmosphere: occurrence, sources and transport. *Sci. Total Environ.* 153794.

Weinberg, I., Dreyer, A., Ebinghaus, R., 2011. Landfills as sources of polyfluorinated compounds, polybrominated diphenyl ethers and musk fragrances to ambient air. *Atmos. Environ.* 45, 935–941.

Worley, R.R., Moore, S.M., Tierney, B.C., Ye, X., Calafat, A.M., Campbell, S., Woudneh, M.B., Fisher, J., 2017. Per- and polyfluoroalkyl substances in human serum and urine samples from a residentially exposed community. *Environ. Int.* 106, 135–143.

Wu, Y., Chang, V.W.C., 2011. The effect of surface adsorption and molecular geometry on the determination of Henry's Law Constants for fluorotelomer alcohols. *J. Chem. Eng. Data* 56, 3442–3448.

Xiao, F., 2017. Emerging poly- and perfluoroalkyl substances in the aquatic environment: a review of current literature. *Water Res.* 124, 482–495.

Yamashita, N., Taniyasu, S., Petrick, G., Wei, S., Gamo, T., Lam, P.K., Kannan, K., 2008. Perfluorinated acids as novel chemical tracers of global circulation of ocean waters. *Chemosphere* 70, 1247–1255.

Zhao, Z., Tang, J., Mi, L., Tian, C., Zhong, G., Zhang, G., Wang, S., Li, Q., Ebinghaus, R., Xie, Z., 2017. Perfluoroalkyl and polyfluoroalkyl substances in the lower atmosphere and surface waters of the Chinese Bohai Sea, Yellow Sea, and Yangtze River estuary. *Sci. Total Environ.* 599, 114–123.